Talanta 121 (2014) 127–135

Contents lists available at ScienceDirect

Talanta

journal homepage: www.elsevier.com/locate/talanta

Nanometer-sized ceria-coated silica–iron oxide for the reagentless microextraction/preconcentration of heavy metals in environmental and biological samples followed by slurry introduction to ICP-OES

A. Dados [a], E. Paparizou [a,c], P. Eleftheriou [b], C. Papastephanou [a], C.D. Stalikas [c,*]

[a] Cp Foodlab, P.O. Box 28729, 2082 Nicosia, Cyprus
[b] Department of Mechanical Engineering, Materials Science and Engineering, Cyprus University of Technology, 3036 Limassol, Cyprus
[c] Department of Chemistry, University of Ioannina, Ioannina 451 10, Greece

ARTICLE INFO

Article history:
Received 31 October 2013
Received in revised form
17 December 2013
Accepted 22 December 2013
Available online 2 January 2014

Keywords:
Nanometer-sized magnetic ceria
Heavy metals microextraction/preconcentration
Slurry suspension sampling
Inductively coupled plasma-optical emission spectrometry

ABSTRACT

A slurry suspension sampling technique is developed and optimized for the rapid microextraction of heavy metals and analysis using nanometer-sized ceria-coated silica–iron oxide particles and inductively coupled plasma optical emission spectrometry (ICP-OES). Magnetic-silica material is synthesized by a co-precipitation and sol–gel method followed by ceria coating through a precipitation. The large particles are removed using a sedimentation–fractionation procedure and a magnetic homogeneous colloidal suspension of ceria-modified iron oxide–silica is produced for microextraction. The nanometer-sized particles are separated from the sample solution magnetically and analyzed with ICP-OES using a slurry suspension sampling approach. The ceria-modified iron oxide–silica does not contain any organic matter and this probably justifies the absence of matrix effect on plasma atomization capacity, when increased concentrations of slurries are aspirated. The As, Be, Mo, Cr, Cu, Pb, Hg, Sb, Se and V can be preconcentrated by the proposed method at pH 6.0 while Mn, Cd, Co and Ni require a pH $\geq$ 8.0. Satisfactory values are obtained for the relative standard deviations (2–6%), recoveries (88–102%), enrichment factors (14–19) and regression correlation coefficients as well as detectability, at sub-μg L^{-1} levels. The applicability of magnetic ceria for the microextraction of metal ions in combination with the slurry introduction technique using ICP is substantiated by the analysis of environmental water and urine samples.

1. Introduction

Nanosized metal oxides, including ferric oxides, manganese oxides, aluminum oxides, titanium oxides, magnesium oxides and cerium oxides provide high surface area and affinity for heavy metals in aqueous systems [1]. These materials are rather unusable in fixed beds or flow-through systems because of the excessive pressure drops, the difficulty of separation from aqueous systems and the poor mechanical strength. On the other hand, magnetic nanosized metal oxides and composite materials attract increasing attention because they can easily be separated from water under a magnetic field, for recycling or regeneration [2].

At analytical scale, the so-called solventless methodologies appear as a green alternative to reduce the volume of solvents used in many sample treatment procedures and, consequently, the volume of toxic wastes produced. Nanometer-sized magnetic particles have attracted interest in the field of analytical chemistry owing to their magnetic and catalytic properties and many researchers have attempted to prepare nanometer-sized magnetic particles with high functionality [3]. In this context, magnetic techniques based on the application of magnetic particles and films have been successfully used for the determination and detection of different types of xenobiotics e.g. herbicides, insecticides, fungicides, aromatic and polyaromatic hydrocarbons and pentachlorophenol [4]. In addition, the versatility and properties of the pristine and functionalized nanometer-scale magnetic materials yielded new and unique applications for the separation and transformation in analytical chemistry for the microextraction of heavy metal ions [5,6].

Ceria (CeO_2) is an attractive metal oxide for many technological applications due to its unique physicochemical properties, including high hardness, chemical inertness, high-temperature strength, and high oxide ion conductivity [7]. The adsorptive properties of ceria vary significantly with morphologies, sizes, shapes and surface areas. The nanoscale effect further induces outstanding properties for nanometer-sized ceria, which has been applied in nanoelectronics [8] as a UV absorbent and a component of

---

Abbreviations: HMT, hexamethylenetetramine; XRD, X-ray diffraction; SEM, scanning electron microscopy; TEOS, tetraethoxysilane; PZC, point of zero charge

* Corresponding author. Tel.: +30 2651008414
E-mail address: cstalika@cc.uoi.gr (C.D. Stalikas).

0039-9140/$ - see front matter © 2013 Elsevier B.V. All rights reserved.
http://dx.doi.org/10.1016/j.talanta.2013.12.045

UV-absorbing coatings [9], in sensors capable of detecting trace impurities in gas mixtures [10,11], in catalysis [12] etc.

Investigation, related to analytical chemistry on the surface chemistry of microscale ceria is scarce but indicates clearly that it may have good adsorption capacity for certain metals [13]. In recent past, it has been shown that hollow nanospheres produced by a template-free microwave-assisted hydrothermal method showed excellent removal capacities for toxic heavy metal ions [14]. A promising approach among the protocols used for ceria particles is the homogeneous precipitation from Ce(III)-hexamethylenetetramine (HMT) solutions. This process is easy to apply and enables synthesis of well-crystallized ceria uniform in particle size, at relatively low temperatures [15]. Besides nanoparticles, ceria has been successfully fabricated in other forms, such as nanorods [16], nanowires [17], nanopolyhedrons [18], three-dimensional flower-like structures [19] and hollow structures [20].

The use of inductively-coupled plasma optical emission spectroscopy (ICP-OES) offers advantages of selectivity, reproducibility and in some cases sensitivity over other atomic spectroscopic methods, but these improvements are always associated with increased efforts in sample pretreatment. In addition, it has to be considered that the elution step after extraction–preconcentration of metals represents a major limitation for the selection of the sorbent material, since only reversible processes can be used for the retention of the analyte on the stationary phase. An alternative to overcome this problem is the introduction of sample slurries into the plasma, which considerably reduces sample preparation time and effort by combining matrix decomposition, analyte atomization and excitation in a single step [21–23].

By definition, “microextraction” is an extraction technique where the volume of the extracting phase is very small in relation to the volume of the sample [24]. The employment of nanometer-sized particles in preconcentration offers a significantly high surface area-to-volume ratio, resulting in high extraction capacity and efficiency and rapid extraction dynamics allowing for microextraction phase to be at considerably small quantity. Besides, the slurry suspension sample introduction technique improves the simplicity, apart from being beneficial for metals interacting irreversibly with the sorbent [25].

In this study, a novel approach is presented for metal analysis, which consists of the following:

(a) synthesis of nanometer-sized magnetic silica by a co-precipitation and sol–gel method followed by the ceria coating through a precipitation from Ce(III)-HMT;
(b) removal of large particles using a sedimentation–fractionation procedure towards producing a magnetic homogeneous colloidal suspension of ceria-modified iron oxide–silica and
(c) metal analysis by ICP-OES using a slurry suspension sampling approach, after magnetic separation of nanometer-sized particles from the sample solution.

The synthesized material is characterized with XRD, FTIR and SEM and is examined for its use for the non-specific microextraction/preconcentration of heavy metals from environmental water samples and biological matrixes.

2. Experimental

2.1. Reagents and standards

Anhydrous iron(III) chloride ≥99.99% trace metals basis, anhydrous iron(II) chloride 99.998% trace metals basis, tetraethoxysilane (TEOS) 99.999% trace metals basis, cerium(III) nitrate hexahydrate and HMT ≥99.5% were obtained from Aldrich (Sigma-Aldrich Hellas). Concentrated nitric acid solution (suprapur 65%) was supplied by Merck (Darmstadt, Germany). Dilute nitric acid solutions were used for slurry suspensions in acidic environment. An ICP multielement stock standard solution (Merck), containing twenty one elements at concentrations of 100 mg L^{-1} and a Hg stock standard solution (Fluka) of 1000 mg L^{-1} were used for the preparation of the final working standards solutions containing the analytes. Aqueous working standard solutions were prepared by appropriate stepwise dilutions of multielement stock standard with 2 N HNO_3. The final working standard solutions had concentrations ranging from few ng L^{-1} to 100 μg L^{-1}, for each analyte, depending on the analyte and the mode of calibration. Finally, a solution containing 2 N HNO_3 was introduced for periodical aspiration and rinsing of the nebulization system. Throughout the work, de-ionized water of 18 MΩ cm^{-1} specific resistance was used, which was obtained from a Millipore Simplicity 185 system.

2.2. Instrumentation

A Thermo Scientific, USA IRIS Intrepid II XDL Thermo Electron Corporation dual viewing inductively coupled plasma atomic emission spectrometer was used, according to the operating conditions (Table S1, Supplementary material). For the measurements, a sensitive, non-interfered emission line per element was used with the instrument set in the axial mode. Transportation of sample solutions to the concentric nebulizer and to the conical spray chamber of the ICP was performed by a peristaltic pump. Sonication was carried out in an Elma low power sonic bath (Elma GmbH & Co, Singen, Germany) with a nominal power output of 50 W. An orbital shaker (Edmund Buhler GmbH, Germany) thermostatted at the desired temperature was employed for stirring of samples.

2.3. Synthesis of nanometer-sized silica magnetic particles

Tetrahydrate iron(III) chloride 0.42 g, hexahydrate iron(II) chloride 1.13 g were mixed in 100 mL of deoxygenated water, under vigorous stirring. The temperature was raised to 80 °C and 5 mL of 25% ammonia was added to form a black precipitate of iron oxide particles. The suspension was further heated for 30 min under continuous flow of nitrogen and the magnetic nanomaterial was separated from the supernatant by a magnet. The solid material was redispersed in de-ionized water, at least three times, until obtaining pH 7, washed twice with ethanol and evaporated to dryness to get 0.5 g of iron oxide powder.

The particles were subsequently coated with TEOS. The procedure consisted of placing 25 mL of ethanol and 8 mL of deionized water into a beaker containing 0.5 g of nanometer-sized iron oxide. Then, 1 mL of ammonia and 500 μL of TEOS were successively added following an overnight stirring, under nitrogen. After magnetic separation, the silanized magnetic particles were thoroughly washed with ethanol.

2.4. Synthesis of nanometer-sized magnetic silica–ceria

The nanometer-sized ceria-modified iron oxide–silica particles were prepared by precipitation of CeO_2 and in-situ formation of the modified nanoparticles from aqueous solutions of cerium(III) nitrate and HTM, as described elsewhere [26]. Final concentrations of 37.5 mM for $Ce(NO_3)_3 \cdot 6H_2O$ (0.326 g) and 0.5 M for HTM (1.6 g) in 20 mL de-ionized water, were mixed with 0.3 g of nanometer-sized magnetic-silica and stirred for 24 h, at 90 °C. The magnetic ceria nanopowder was obtained by applying an external magnetic field and after washing with de-ionized water and ethanol the nanomaterial was oven dried.

2.5. Preparation of ceria dispersion

For the preparation of ceria dispersion, the dried magnetic silica–ceria material was first ground with an agate mortar and pestle and then added to de-ionized water and sonicated in an ultrasound bath cleaner, for 20 min. The initial concentration of ceria was 1.0 mg mL^{-1}. During sonication, the temperature in the dispersion rises up to 40 °C. After sonicaton, the obtained dark orange dispersion was let stand undisturbed for 1 h, for sufficient sedimentation of the large particles. The upper less dark dispersion was collected and centrifuged at 1000 rpm for 5 min with a Hettich Universal centrifuge (Hettich GmbH Tuttlingen, Germany) to remove any large particles, thus resulting in a magnetic homogeneous colloidal aqueous suspension of ceria modified silica–iron oxide. For the separation of particles, a conventional magnet was applied and after the removal of the bulk water and drying in an oven at 90 °C, the solid nanometer-sized material was calculated by the weight method. Finally, the concentration of the suspension was adjusted to 2 mg mL^{-1}.

2.6. Microextraction/preconcentration of metals and analysis

Aqueous samples with varying initial metal concentrations were prepared by dilution of the stock standard solution with de-ionized water. All the experiments were carried out in 100 mL capped bottles containing 50 mL of standard solution (or sample) at 25 °C and the nanometer-sized material was added in the form of a suspension, prepared by dispersing the synthesized product in de-ionized water, as described above. The initial pH values of the solutions were adjusted to 6.0 or 8.0 by addition of 0.1 N HNO_3 or 0.1 N NaOH. The procedure was carried out in a contact time period of 30 min with the concentration of nanometer-sized particles to be at 5 mg per 50 mL of sample. Stirring was maintained at 300 rpm to disperse the particles throughout the sample and to ensure quantitative extraction using an orbital shaker. Once equilibrium was reached, the nanosorbent with the retained analytes was harvested via an external magnetic field for metal analysis. The remaining particles were washed with de-ionized water and used for the preparation of slurry, after dispersion of the sorbent in 2.5 mL of 2 N HNO_3, under ultrasonication. For ICP-OES measurements, the slurry was directly introduced into the plasma, where first the particles were disintegrated and second the target analytes were atomized and excited. During sample aspiration, slurry was continuously ultrasonicated. Between aspirations of the suspensions, a 2 N HNO_3 solution flushed the nebulizer–torch system to remove any residual sample, prevent clogging and minimize the chance of any possible memory effect.

2.7. Characterization of the nanomaterial

The X-ray diffraction (XRD) analysis of the dispersed, isolated and dried material was carried out on a D8 Advance diffractometer from Bruker AXS (Madison, USA) using Cu Kα radiation. Particle shape and diameter were assessed by scanning electron microscopy (SEM) images taken on a JEM-2010F (JEOL Ltd., Japan) by drop casting the dispersion onto a copper strip.

The surface area was characterized using an Autosorb-1 porosimeter from Quantachrom Instruments (Boynton Beach, USA). The BET surface area was 133 $m^2\,g^{-1}$. The point of zero charge (pH_{PZC}) of the nanometer-sized material was determined using a procedure described elsewhere [5].

The FT-IR spectra were recorded on a Perkin-Elmer Spectrum GX FT-IR spectrophotometer with samples as KBr pellets. The KBr wafers were prepared by mixing KBr crystals with sample, dried previously at 100 °C for 24 h and ground to fine powder.

Elemental analysis of Si and Ce in the prepared composite nanoscale material was carried out with ICP-OES. For the determination of Si, the solid sample was treated with 5 mL of 0.1 N NaOH, sonicated for 1 min, diluted to 10 mL with de-ionized and acidified with concentrated nitric acid. The Ce content was determined after treatment with 5 mL of 2 N HNO_3 and heating at 50 °C, for 1 h.

Magnetization measurements were collected at room temperature using a Vibrating Sample Magnetometer (LakeShore 7300, Westerville, OH, USA).

3. Results and discussion

3.1. Synthesis and characterization of the composite nanomaterial

The FT-IR measurements for iron oxide–silica and CeO_2-coated iron oxide–silica nanometer-sized particles were conducted and the spectra are shown in Fig. 1. Residual water is detected with a large band around 3400 cm^{-1}, corresponding to O–H stretching frequency and a broad band at 1600 cm^{-1}, due to the bending vibrations of the associated water. The band of Si–O–Si asymmetric stretching vibration in iron oxide–silica appears at around 1100 cm^{-1}. This band shifts to lower wavenumber after coating with CeO_2, probably because of the influence of this material on the structure of SiO_2. Comparing the spectra of iron oxide–silica and CeO_2-coated iron oxide–silica, among others, the presence of a new band at 965 cm^{-1} is evident. This band has been reported to arise from Ce–O–Si vibration [27]. In addition, Fig. 2 shows that in XRD patterns the phases of iron oxide, ceria and iron oxide hydroxide are visible.

The diameters of the quasi-spherical particles of the produced slurry as they appear in the SEM micrographs range from 100 to 250 nm (Supplementary material Fig. S1). The presence of iron, silicon and cerium was also confirmed by EDS analysis (Supplementary material Fig. S2). Finally, the elemental analysis using ICP-OES, yielded 9% Si and 24% Ce contents, which are in good agreement with the EDS data. The saturation magnetization of the nanometer-sized material was 48 A m^2/kg (Supplementary material Fig. S3). It seems that the material retains its magnetic properties even after the two coatings on iron oxide. Complete magnetic separation is achieved in 1 min by applying a magnetic field (B-field=0.25 T) near the tube which contains the aqueous dispersion of the material.

The pH_{PZC} is located at 6.9 (Supplementary material Fig. S4); the surface charge of the material remains negative above the pH_{PZC} and positive below this value. The pH_{PZC} of silica coated iron oxide is close to 3, as demonstrated in our previous study [5]. The respective value of CeO_2 has been reported to be around 6.9 [28]. The synthesized material displays a value significantly shifted from that of iron oxide–silica toward that of pure CeO_2. This indicates that the shell of CeO_2 is almost complete and iron oxide–silica in the core may not exert a significant effect on the charge of the composite material.

3.2. Study and optimization of the enrichment procedure

A screening and optimization study has been performed to assess the capacity of the nanomaterial to interact with metal ions and to come up with the best performance conditions. To optimize the designed procedure and set the criteria of selection, several factors were isolated from the different stages of analysis (i.e. pH, extraction time and temperature, sample volume, slurry amount and state and ICP-OES measurement) and carefully investigated with synthetic aqueous sample solutions. For method development, initial conditions with a sample volume of 50 mL and

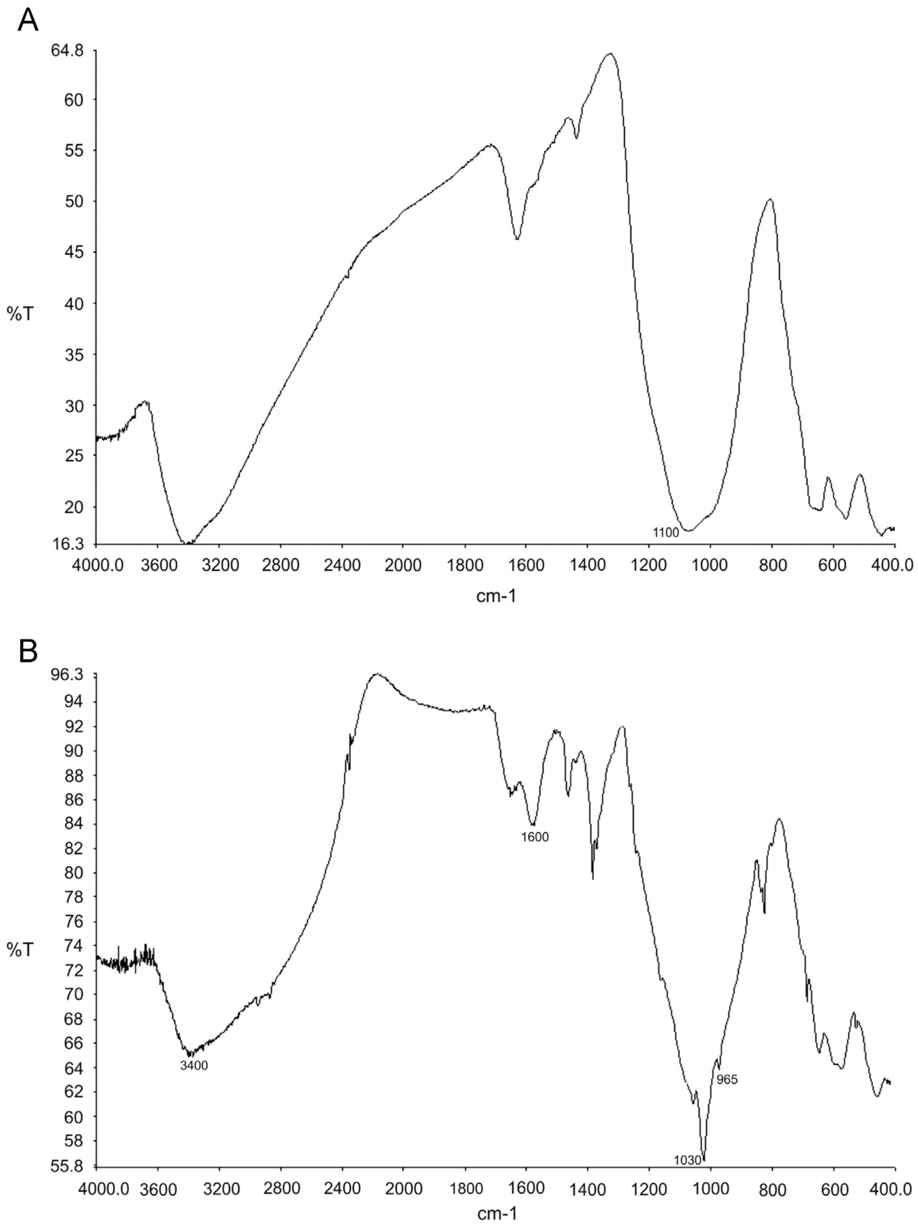

Fig. 1. FT-IR spectra of iron oxide–silica (A) and ceria-coated iron oxide–silica (B).

concentration of 2.0 μg L^{-1} for each metal have been used. Regarding the amount of the synthesized nanometer-sized material, 2.5 mL of a suspension containing 5 mg of particle mass per sample were added to the sample solution. All investigations were carried out with three-fold replication.

3.2.1. Effect of pH

The initial pH values of the solutions were adjusted to 3.0–10.0 by addition of 0.1 N HNO_3 or 0.1 N NaOH. Based on the initial concentration of metal ions like Ni, Cd, Co, Cu, Pb and the solubility-product constants (K_{sp}) of the respective hydroxides, the pH value where hydroxyl complexes precipitate is expected to be greater than 10. Hence, it is reasonable to consider this value to be the upper limit in the pH range studied.

The pH plays a determining role to the sorption of different ions on oxide surfaces. As a rule, adsorption of cations on amphoteric oxides including ceria, proceeds when the pH value of the solution is higher than pH_{PZC} of oxide, whereas for anion adsorption a pH value lower than the pH_{PZC} is required. In our study, an increase in pH is generally accompanied by an increase in the percent of extracted metals. More specifically, the results demonstrate the capacity of nanometer-sized ceria magnetic particles to efficiently adsorb and therefore concentrate simultaneously As, Be, Cr, Cu, Mo, Hg, Pb, Sb, Se and V over a wide range of pH from 5.0 to 8.0 (Fig. 3). Among them, As, Cr, Sb, Mo, V and Se appear in the solutions as oxyanions and their specific forms depend on the pH. Except for Mo, the metals are extracted at high percents in a broad pH range, exhibiting a slight tendency for reduction as the pH increases above the pH_{PZC}, where the surface charge turns negative. In the pH interval between 9.0 and 10.0, Mn, Cd, Co and Ni can also be preconcentrated in high yield. Evidently, a single pH value where the extraction efficiency acquires simultaneously a maximum for all metals studied does not exist. However, it has been demonstrated that it is reasonable to maintain the pH as close to the pH_{PZC} as possible when working with metal oxides due to the propensity of unbuffered suspensions of such nanomaterials to drift into their pH_{PZC}, in the course of

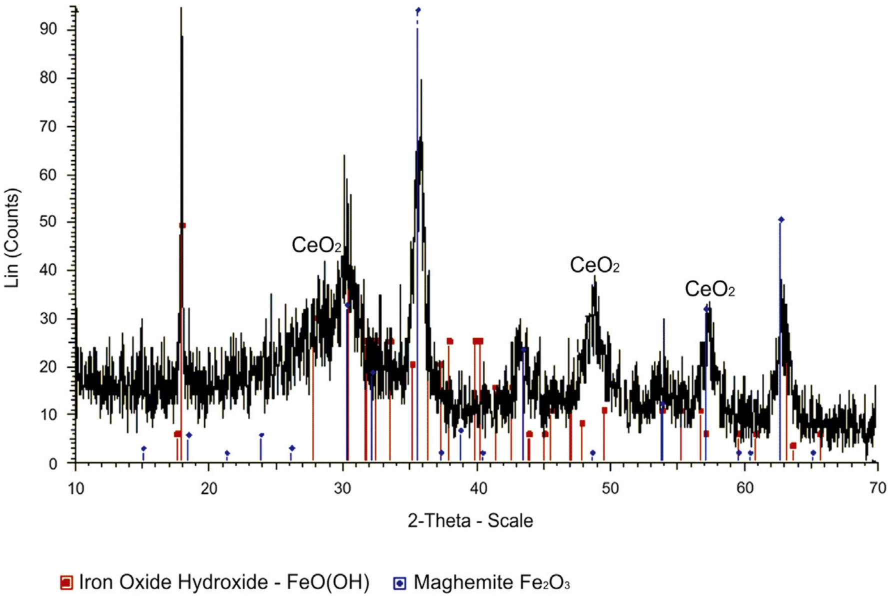

Fig. 2. XRD diffractogram of ceria-coated silica–iron oxide.

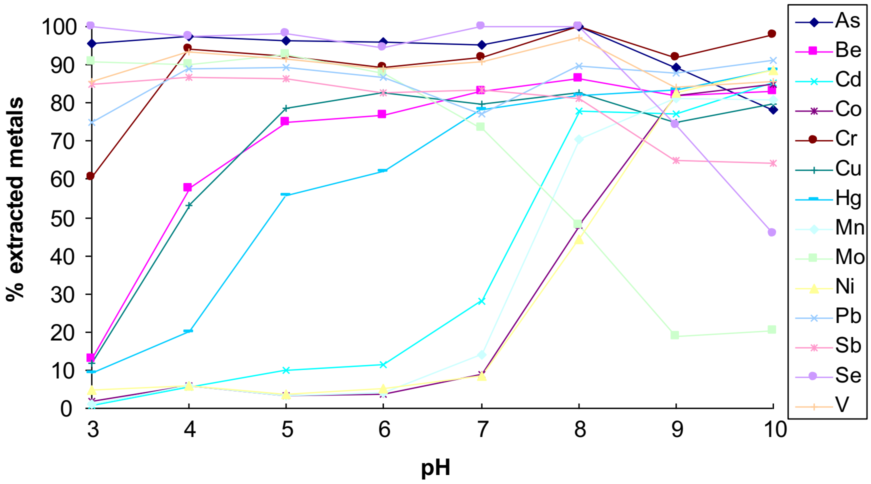

Fig. 3. Effect of pH on the extraction of metals on ceria-coated silica–iron oxide.

time [6]. This, additionally, negates the need of preparing and using buffer solutions, which add steps in the preconcentration and potential risk of higher blank values. As a compromise, the pH value of 7.0 was selected for the subsequent experiments, which satisfies the preconcentration requirement for most of the metals studied. Whereas pH 8.0 is not the optimal especially for Co and Ni, it can be recommended for Mn, Cd, Co and Ni since it is close to the pH_{PZC}.

3.2.2. Sorption kinetics

The time-dependent behavior of the nanoscavenger extraction efficiency for heavy metals was measured by varying the equilibrium contact time up to 120 min, at a stirring rate of 300 rpm. The amount of the added magnetic ceria dose was 5 mg per 50 mL of sample. Displayed in Fig. 4 are the kinetic curves of the selected heavy metals adsorbed onto ceria nanoscavenger. The retention trend for the metals studied seems to be almost alike at both pH values, i.e. at and above the pH_{PZC}, except for Ni and Co, which do not acquire plateau even after 120 min. It is interesting to note that the uptake of most of the metals from the nanosorbent increases sharply within the first 10 min acquiring equilibrium before 30 min. Leaching of the metals from the sorbent does not occur after that particular period of time.

The extraction process is rapid in the first few minutes during which the rate of the uptake of metal ions from the solution is significantly faster than at later times. This behavior of the high initial rate of uptake, which is followed by a plateau, occurs almost regardless of the metallic species and hints at a physical rather than a chemical mechanism.

3.2.3. Slurry conditions and sample volume

The elution step after preconcentration of metals on a sorbent represents a major limitation for the selection of it, since only reversible processes can be used for the retention of the analyte on the stationary phase. The ceria-coated silica–iron oxide exhibited strong interaction with certain metals like As, Sb and Cu to such an extent that elution under strongly acidic conditions is ineffective and under alkaline conditions is only partial. To overcome this problem, the introduction of sample slurry into the plasma is a potential solution. It is known that the particle diameter affects the efficiency of sample introduction as well as the excitation capabilities in plasma. A prerequisite for the successful application

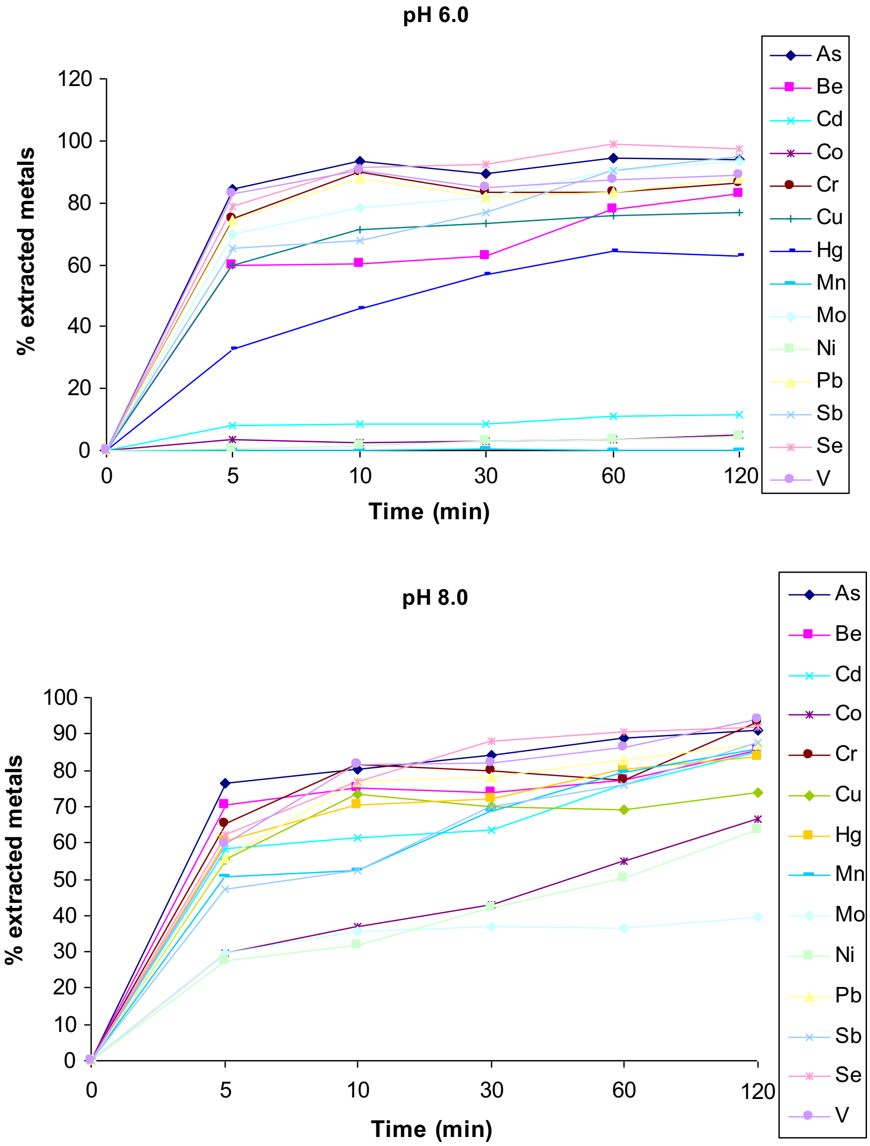

Fig. 4. Percent of extracted metals as a function of time, at pH 6.0 and pH 8.0.

of the developed slurry approach is the use of sorbent particles with as low as possible mean particle size. The particle size of the slurry deriving from the relevant procedure was smaller than 250 nm and the stability of slurry was ensured by a continuous ultrasonication during aspiration. The use of ultrasonication was more effective than continuous stirring as the within-sample reproducibility of ICP-OES signal was less than 1% and no precipitation was formed in the delivery tube, at the optimum concentration of the suspension. The sedimentation–fractionation procedure, which followed the synthesis of the material, resulted in the control of particle size avoiding the introduction of large particles or formation of agglomerates during ICP-OES measurements.

To achieve an optimum of the amount of nanosized material, their introduced amount was varied from 1 to 10 mg per sample. That is necessary for the quantitative enrichment and study of signal suppression during ICP-OES analysis due to a decrease in plasma excitation capabilities. Emission signals increased steadily until the content of the material reaches the 2.5 mg per sample. Increasing the amount of particles above 5 mg per sample, resulted in frequent clogging of the ICP aspiration line and in fluctuation in the emission signals due to discontinuities in sampling. The gradual enhancement with the increase in the particle content can reasonably be explained by the increasing number of surface active sites available for the analytes. All subsequent investigations were carried out with a particle amount of 5 mg per sample to compensate for higher concentrations of metal ions in real samples.

The volume of multielement containing solution with a concentration of 2.0 μg L^{-1} was varied from 10 to 100 mL to test the linearity of the enrichment procedure with a constant particle mass of 5 mg per sample and a final volume of 2.5 mL after pretreatment. Between the measured signal intensities and the applied sample volumes up to 50 mL, a linear correlation was noticed for all studied metals, indicating that the retention capabilities of the nanometer-sized particles were not limited up to the abovementioned volume. Higher volumes are not preferable due to the high dispersion of the particles in the bulk solution and extraction efficiencies are apt to diminish.

Finally, with a resuspending volume of 2.5 mL, the optimal conditions were established, achieving high signal intensities, acceptable standard deviations and therefore reproducible sample pretreatment with low risk of clogging of the aspiration system of ICP-OES. The final volume of 2.5 mL which has been used, results in a theoretical enrichment factor of 20 considering a 50-mL initial volume.

3.2.4. *Effect of stirring rate and temperature*

Sample agitation is known to enhance extraction by way of accelerating the mass transfer of the analytes. An increase in extraction efficiency by 20–40% was observed for the metals studied as the stirring rate rose to 300 rpm (this value being the highest possible setting, under the instrumental limitations). Especially, a steep increase in the extraction of some metals was noticed increasing the stirring rate from 150 to 250 rpm, signifying the strong influence of mass transfer rate of metals to the nanosorbent. A stirring rate of 300 rpm was finally adopted.

The temperature in the studied range of 25–45 °C has no significant bearing on the extraction efficiency. Diffusion is an endothermic process and the lack of any enhancement of retention efficiency with temperature provides no evidence for a pore diffusion-controlled retention process of metallic species on ceria. A temperature of 25 °C ensures a considerable uptake for all metals studied.

3.2.5. *Effect of ionic strength, foreign inorganic ions and humic acids*

The effect of ionic strength on the retention of heavy metals was studied using solutions of NaCl, at pH 6.0 and 8.0. The concentration of NaCl up to 500 mM showed negligible change in the uptake of As, Cr, Sb and Se. This behavior of the oxyanion-forming metals is probably attributed to the weakness of chloride to compete with them for the adsorption sites of magnetic ceria even at high concentrations of salt. In contrast, a negative effect becomes gradually important, for the rest of the metals as the NaCl content is getting greater than 10 mM, thus signifying a considerable interference, under these conditions. It is concluded that under high salinity conditions, the material is usable only for the microextraction of As, Cr, Sb and Se. Nonetheless, a nanomaterial-based microextraction method can be practical and effective over a wide range of metals in most of the environmental water samples.

The presence of other ionic species could provoke competition for the sorption sites of magnetic ceria and hamper analyte retention on the nanometer-sized particles. In this context, standard solutions of the heavy metals studied were fortified with the chloride salts of Ca, Mg and Al, at three spiking levels for each of them. More exactly, the concentration levels were 20, 100 and 200 ppm for Ca, 10, 50 and 100 ppm for Mg and 50, 200 and 1000 ppb for Al, which are within the range or well above the concentrations found in ground water, surface water and urine. No interference was observed for the above metals ions at any concentration level. The overwhelming excess of the nanomaterial in the extraction medium can guarantee the absence of interference.

Another issue, which is also worth studying for practical applications, is the effect of humic acid due to its occurrence in natural waters. The interaction of the material with humic acid results in a polyanionic organic coating on metal oxides, essentially altering the surface properties of the particles. The experiments performed revealed that the presence of humic acid up to 10 mg L^{-1} caused practically no alteration to the retention of metals. Normally, the concentration of humic acid in freshwaters is lower than the maximum values examined in this work [29] indicating that no interference is foreseen when the method is to be applied to real-life aqueous samples.

3.2.6. *Calibration curves*

The effect of nanometer-sized magnetic ceria during enrichment and measurement can become obvious when comparing the slopes of different calibration approaches. Five-point calibration curves were drawn for the most sensitive spectral line of each analyte, using aqueous standard solutions and slurry suspension standards. Multielement calibration standards were used for all metals. The slurry suspension standards were made by adding 5 mg of the nanomaterial to 2.5 mL of standard solutions prepared in 2 N HNO_3. A blank slurry suspension without the spiking of any metal was also prepared.

The sensitivity of each calibration is expressed by the slope of the linear regression equation. The slopes together with their corresponding standard errors, the linear correlation coefficients and the analytical line for all metal ions are presented in Table 1. The calculated slopes for the aqueous standard calibrations are very similar to those obtained by the developed slurry suspension procedure (two-tailed *t*-test, $P=0.05$) with the exceptions of Cd and Cu, thus indicating unchanged sensitivity when the slurry is present. This also provides evidence that matrix effect on plasma atomization capacity is not influential enough to alter the total performance of the method, when increased concentrations of slurries are aspirated. It has been established that the introduction of organic matrix slurries into the plasma atomizer deteriorates the atomization capability, restricting significantly the applicability of the technique [30]. The ceria-modified iron oxide–silica, by its very nature, has the edge over a multitude of other sorbents of not containing organic matter. Satisfactory values were also obtained for the correlation coefficients of regression, indicating the acceptable linearity in the studied range with the exception of Cr and Hg (Table 1). Although Fe is line-rich element, the introduction of the nanometer-sized particles into the ICP in slurry form appears not to result in serious spectral interferences. Cadmium is the exception because it emits a spectral line (226,502 nm) very close to one of the plenty of Fe (226,505 nm) with an intensity ratio of Cd/Fe=1071 [31]. This probably explains the difference noticed in the slopes of calibration curves of Cd constructed in aqueous standard and slurry suspension, as discussed above.

3.2.7. *Analytical figures of merit and applicability*

The quantitation limits for the determination of the investigated metals – based on ten times the standard deviation of five blank solutions – are given in Table 2 and confirm the applicability, at sub-μg L^{-1} levels. The precision of the proposed slurry suspension microextraction method was evaluated by calculating the relative standard deviation obtained for five repetitive determinations of a 1.0 μg L^{-1} multielement solution and ranged from 2% for Be to 6% for Sb.

The enrichment factors, defined as the ratio between the analyte concentration in the enriched solution and in the original one, are provided in Table 2. Considering the high signal intensity, as already described and the effective extraction of most of the

Table 1
Spectral lines of ICP-OES measurements, values of slope ± standard error of the calibration curves and correlation coefficients.

Analyte	Spectral line	Slope of aqueous standard calibration	Slope of slurry suspension calibration	Correlation coefficient
As	189.042	0.04 ± 0.01	0.04 ± 0.01	0.9989
Be	313.042	0.67 ± 0.02	0.65 ± 0.03	0.9996
Cd (pH 8)	226.502	0.73 ± 0.02	0.80 ± 0.03	0.9996
Co (pH 8)	228.616	1.41 ± 0.05	1.31 ± 0.07	0.9999
Cr	267.716	0.20 ± 0.02	0.18 ± 0.02	0.9962
Cu	324.754	0.48 ± 0.02	0.55 ± 0.03	0.9989
Hg	184.950	0.08 ± 0.01	0.08 ± 0.01	0.9945
Mn (pH 8)	257.610	1.20 ± 0.05	1.17 ± 0.06	0.9999
Mo	202.030	0.39 ± 0.02	0.35 ± 0.03	0.9989
Ni (pH 8)	221.647	0.68 ± 0.03	0.74 ± 0.04	0.9987
Pb	220.353	0.06 ± 0.01	0.05 ± 0.01	0.9983
Sb	206.833	0.08 ± 0.01	0.08 ± 0.01	0.9989
Se	196.090	0.05 ± 0.02	0.06 ± 0.01	0.9985
V	292.402	0.08 ± 0.02	0.07 ± 0.02	0.9997

Table 2
Limits of quantitation and preconcentration factors for the studied metals using the slurry suspension sampling of ceria-coated silica–magnetite nanoparticles.

Analyte	LOQ (μg L^{-1})	Preconcentration factor
As	0.46	18
Be	0.15	19
Cd (pH 8)	0.05	18
Co (pH 8)	0.12	14
Cr	0.61	18
Cu	0.51	17
Hg	0.10	16
Mn (pH 8)	0.14	18
Mo	0.22	14
Ni (pH 8)	0.14	14
Pb	0.51	17
Sb	0.29	19
Se	0.24	19
V	0.23	19

Table 3
Mean concentrations ($n=3$) of metals in environmental and biological samples (μg L^{-1}).

Analyte	Well water*	Reservoir water*	Urine**
As	3.0 ± 0.2	3.0 ± 0.3	3.2 ± 0.3
Be	0.40 ± 0.01	0.051 ± 0.02	0.70 ± 0.02
Cd (pH 8)	0.39 ± 0.02	0.20 ± 0.01	0.6 ± 0.2
Co (pH 8)	0.21 ± 0.03	0.21 ± 0.03	nd
Cr	0.12 ± 0.01	nd	4.1 ± 0.2
Cu	4.7 ± 0.3	8.3 ± 0.3	5.1 ± 0.3
Hg	nd	nd	nd
Mn (pH 8)	1.1 ± 0.2	1.4 ± 0.3	0.9 ± 0.1
Mo	1.9 ± 0.1	1.3 ± 0.1	4.9 ± 0.3
Ni (pH 8)	19.7 ± 0.9	3.2 ± 0.2	nd
Pb	3.4 ± 0.2	3.2 ± 0.2	nd
Sb	4.3 ± 0.3	2.2 ± 0.2	nd
Se	20 ± 1	2.1 ± 0.1	23 ± 1
V	23 ± 1	7.2 ± 0.3	nd

* Water samples received from Nicosia, Cyprus.
** Donated by a healthy female (smoker) volunteer.

metals, satisfactory enrichment factors are anticipated, which guarantee higher sensitivity. The calculated factors ranged from 14 for Mo, Co and Ni to 19 for Sb, Se, V and Be. In order to test the applicability of the proposed method, well water and reservoir water samples as well as a urine sample were collected and analyzed without any pretreatment. The results, as the average of three separate determinations, are shown in Table 3. The accuracy was evaluated by determining the recoveries of the analytes from environmental and biological matrixes spiked at two concentration levels of three and five times the quantitation limits for each metal. The recoveries obtained after the slurry suspension for most of the analytes ranged between 88% and 102%. Less satisfactory, close to 88%, were the recoveries for Hg, Ni, Co and Mn.

Other magnetic metal oxide-based non-functionalized nanosorbents have been proposed in the literature for the removal of metals from water samples. It has been reported that magnetite can adsorb Pb [32], Cr, Cd, Cu, Zn, and Ni [33] and Pb, Cu, Zn and Mn [34] and mixed magnetite–hematite nanoparticles and nanoscale Fe/Fe_2O_3 are suitable for Pb, Cd and Cr(III) [35] and Cd, Pb, Ni, Cr(VI) and As(V) [6], respectively. A MnO_2-coated magnetic nanocomposite exhibit improved removal capacity toward Cd, Cu, Pb and Zn compared to unmodified magnetite nanoparticles [36] while manganese-doped iron oxide nanoparticles have a remarkably high affinity for Co, Ni, Zn, As, Ag, Cd, Hg and Tl compared to the precursor material [37]. From the analytical point of view, magnetite–silica–titania nanoparticles has been developed using a two-step method for the separation/preconcentration of trace amounts of Cd, Cr, Mn and Cu in environmental water samples followed by inductively coupled plasma mass spectrometry (ICP-MS) detection [38]. All the above materials deal with the removal or preconcentration of heavy metals, they could be potential candidates for slurry introduction since they are not organic-based matrixes, but they have been reported to be applied for a less number of metals as compared to the present study.

4. Conclusion

A novel microextraction/preconcentration procedure for the multielement enrichment of As, Be, Mo, Cr, Cu, Pb, Hg, Sb, Se, V, Mn, Cd, Co and Ni has been introduced prior to analysis with ICP-OES. The procedure combines the magnetic and metal extracting properties of a non-specific nanometer-sized ceria–iron oxide–silica with a slurry suspension sampling approach and ICP-OES slurry measurement. It has been demonstrated that the effects due to the introduction of particles into the plasma are absent and satisfactory enrichment capabilities of the nanomaterial are attained. The method is characterized by simplicity and low cost of analysis and shows distinct advantages for nanosorbent handling and memory effects by implementing the slurry sampling, negating the need for re-extraction of metals. This feature of the developed procedure establishes access to (nano)sorbents with irreversible bonding mechanisms for sample pretreatment. The proposed method requires minimal sample preparation and offers good detection limits and acceptable precision for routine analysis of liquid environmental and biological samples. Conceivably, the detection limits can further be improved using higher content of sorbent in the slurries in combination with higher sample volumes but with a reasonable sacrifice to the precision of the final slurry measurement.

Acknowledgments

This work was funded by the Republic of Cyprus (Research Promotion Foundation) and the EU Structural Funds under the program “Functionalized magnetic nanocomposites in conjuction with atomic spectroscopy for the improved trace determination of heavy metals: Nano-Spectroscopy”. The use of the XRD and SEM units of the Network of Research Units of the University of Ioannina is gratefully acknowledged.

Appendix. Supplementary material

Supplementary data associated with this article can be found in the online version at http://dx.doi.org/10.1016/j.talanta.2013.12.045.

References

[1] M. Hua, S. Zhang, B. Pan, W. Zhang, L. Lv, Q. Zhang, J. Hazard. Mater. 211–212 (2012) 317–331.
[2] R.D. Ambashta, M. Sillanpää, J. Hazard. Mater. 180 (2010) 38–49.
[3] K. Aguilar-Arteaga, J.A. Rodriguez, E. Barrado, Anal. Chim. Acta 674 (2010) 157–165.
[4] I. Safarik, K. Horska, K. Pospiskova, M. Safarikova, Anal. Bioanal. Chem. 404 (2012) 1257–1273.
[5] A.E. Karatapanis, Y. Fiamegos, C.D. Stalikas, Talanta 84 (2011) 834–839.
[6] A.E. Karatapanis, D.E. Petrakis, C.D. Stalikas, Anal. Chim. Acta 726 (2012) 22–27.
[7] B.N. Kilbourn, Cerium: A Guide to Its Role in Chemical Technology, Molycorp, New York (1995) 42.
[8] X. Feng, D.C. Sayle, Z.L. Wang, Science 312 (2006) 1504–1508.
[9] A. Corma, P. Atienzar, H. Garcia, J.Y. Chane-Ching, Nat. Mater. 3 (2004) 394–397.
[10] N. Izu, W. Shin, Sens. Actuators B 113 (2006) 207–213.

[11] W.C. Maskell, Solid State Ion. 134 (2000) 43–50.
[12] A. Trovarelli, C. de Leitenburg, M. Boaro, G. Dolcetti, Catal. Today 50 (1999) 353–367.
[13] E. Vassileva, B. Varimezova, K. Hadjiivanov, Anal. Chim. Acta 336 (1996) 141–150.
[14] C.-Y. Cao, Z.-M. Cui, C.-Q. Chen, W.-G. Song, W. Cai, J. Phys. Chem. C 114 (2010) 9865–9870.
[15] F. Zhang, Q. Jin, S.-W. Chan, J. Appl. Phys. 95 (2004) 4319–4326.
[16] X.W. Liu, K.B. Zhou, L. Wang, B.Y. Wang, Y.D. Li, J. Am. Chem. Soc. 131 (2009) 3140–3141.
[17] T.Y. Yu, J. Joo, Y.I. Park, T. Hyeon, Angew. Chem. Int. Ed. 44 (2005) 7411–7414.
[18] R. Si, Y.W. Zhang, L.P. You, C.H. Yan, Angew. Chem. Int. Ed. 44 (2005) 3256–3260.
[19] L.S. Zhong, J.S. Hu, A.M. Cao, Q. Liu, W.G. Song, L.J. Wan, Chem. Mater. 19 (2007) 1648–1655.
[20] N.C. Strandwitz, G.D. Stucky, Chem. Mater. 21 (2009) 4577–4582.
[21] Q.Z. Bian, P. Jacob, H. Berndt, K. Niemax, Anal. Chim. Acta 538 (2005) 323–329.
[22] E.J. dos Santos, A.B. Herrmann, V.L.A. Frescura, A.J. Curtius, Anal. Chim. Acta 548 (2005) 166–173.
[23] B. Kollander, M. Andersson, J. Pettersson, Talanta 80 (2010) 2068–2075.
[24] C.D. Stalikas, Y.C. Fiamegos, Trends Anal. Chem. 27 (2008) 533–542.
[25] G. Bauer, M.-A. Neouze, A. Limbeck, Talanta 103 (2013) 145–152.
[26] P.L. Chen, I.W. Chen, J. Am. Ceram. Soc. 76 (1993) 1577–1583.
[27] X. Song, N. Jiang, Y. Li, D. Xu, G. Qiu, Mater. Chem. Phys. 110 (2008) 128–135.
[28] R. Manivannan, S. Ramanathan, Appl. Surf. Sci. 255 (2009) 3764–3768.
[29] D.D. Anagnostou, Y.C. Fiamegos, C.D. Stalikas, Int. J. Environ. Anal. Chem. 92 (2012) 1239–1250.
[30] G.A. Zachariadis, A.F. Olympiou, J. Pharm. Biomed. Anal. 47 (2008) 541–546.
[31] A. Kramida, Y. Ralchenko, J. Reader, NIST ASD Team, NIST Atomic Spectra Database (ver. 5.1), National Institute of Standards and Technology, Gaithersburg, MD, 2013.
[32] B. Zou, Y. Liu, Y. Wang, RSC Adv. 45 (2013) 23327–23334.
[33] E. Matei, A.M. Predescu, C. Predescu, M.G. Sohaciu, A. Berbecaru, C.L. Covaliu, J. Environ. Qual. 42 (2013) 129–136.
[34] L. Giraldo, A. Erto, J.C. Moreno-Piraján, Adsorption 19 (2013) 465–474.
[35] M.A. Ahmed, S.M. Ali, S.I. El-Dek, A. Galal, Mater. Sci. Eng. B 178 (2013) 744–751.
[36] E.-J. Kim, C.-S. Lee, Y.-Y. Chang, Y.-S. Chang, ACS Appl. Mater. Interfaces 19 (2013) 9628–9634.
[37] C.L. Warner, W. Chouyyok, K.E. Mackie, D. Neiner, L.V. Saraf, T.C. Droubay, M.G. Warner, R.S. Addleman, Langmuir 28 (2012) 3931–3937.
[38] N. Zhang, H. Peng, B. Hu, Talanta 94 (2012) 278–283.